

RSC Advances



This is an *Accepted Manuscript*, which has been through the Royal Society of Chemistry peer review process and has been accepted for publication.

Accepted Manuscripts are published online shortly after acceptance, before technical editing, formatting and proof reading. Using this free service, authors can make their results available to the community, in citable form, before we publish the edited article. This *Accepted Manuscript* will be replaced by the edited, formatted and paginated article as soon as this is available.

You can find more information about *Accepted Manuscripts* in the [Information for Authors](#).

Please note that technical editing may introduce minor changes to the text and/or graphics, which may alter content. The journal's standard [Terms & Conditions](#) and the [Ethical guidelines](#) still apply. In no event shall the Royal Society of Chemistry be held responsible for any errors or omissions in this *Accepted Manuscript* or any consequences arising from the use of any information it contains.

Nanocrystalline $\text{Ni}_{0.8}\text{Zn}_{0.2}\text{Fe}_2\text{O}_4/\text{SrFe}_{12}\text{O}_{19}$ Composite Fiber with Enhanced Exchange Coupling Behavior

Xianfeng Meng*, Tong Liu, Le Yu, Kai Jin, Song Xu

School of Materials Science and Engineering, Jiangsu University, 301 Xuefu Road, Zhenjiang 212013, China

Corresponding author: Xianfeng Meng (mxmf2029@mail.ujs.edu.cn)

Abstract

Exchange coupled nanocrystalline $\text{Ni}_{0.8}\text{Zn}_{0.2}\text{Fe}_2\text{O}_4$ (NZFO)/ $\text{SrFe}_{12}\text{O}_{19}$ (SFO) composite fibers were successfully fabricated using the sol-gel spinning technique followed by annealing. Pure phase nanocrystalline composite fibers, consisting of magnetically soft NZFO and hard SFO phases, were obtained at 900 °C for 2 h in air. The results showed that the magnetic properties of NZFO/SFO composite fibers strongly depended on annealing temperature. At the annealing temperature of 900 °C, the hysteresis loop of NZFO/SFO composite fiber showed a single-phase-like magnetic characteristic, indicating existence of effective exchange coupling between the NZFO phase and the SFO phase. The saturation magnetization (M_s), coercive force (H_c) and remanence (M_r) increased initially, reaching their maximum values at 1000 °C. However, further increasing annealing temperature to 1100 °C, a constrictive hysteresis loop appeared which implied the reduction of exchange coupling interaction and therefore decreased magnetic properties of NZFO/SFO composite fibers.

Keywords: sol-gel spinning, nanocrystalline fiber, soft/hard magnetic, exchange coupling

1. Introduction

Nanocomposite magnets based on exchange spring mechanism have captured intensive

attention, mainly because of the prediction of energy product $(BH)_{\max}$ in excess of 100 MGOe [1-3]. The realization of such high $(BH)_{\max}$ is grounded on the beneficial combination of the large specific saturation magnetization of the soft phase and the high coercive field of the hard phase [4-6]. For reaching an optimum exchange coupling effect between soft phase and hard phase, in the past few decades, a number of studies have been carried out on Nd-Fe-B and Sm-Co based nanocomposite magnets [7-10]. Unfortunately, up to now, the energy product of nanocomposite magnets is still a big discrepancy compared with the expected theoretical value, because of difficulties in controlling the nanostructures in nanocomposite bulk magnets.

Recently, considerable attention has been paid to the exchange-spring effect in soft/hard ferrite nanocomposite. The composite consists of magnetically soft spinel type and hard magnetoplumbite type ferrites. Roy et al [11] prepared the exchange spring nanocomposite particles involving soft ferrite ($\text{Ni}_{0.8}\text{Zn}_{0.2}\text{Fe}_2\text{O}_4$) and hard ferrite ($\text{BaFe}_{12}\text{O}_{19}$) which were mixed in certain weight ratio. They found exchange spring behavior with a maximum coercivity of 88 kA/m for the 1:4 weight ratio. Hoque et al [12] discussed exchange spring mechanism of $\text{Co}(\text{Mg})\text{Fe}_2\text{O}_4/\text{BaFe}_{12}\text{O}_{19}$ nanocomposites, revealing convex hysteresis loops characteristic of single-phase permanent magnet in soft/hard nanocomposites. However, the reported investigations on soft/hard ferrite nanocomposites have mainly focused on nanoparticle and multilayer film. Less work has been done on one-dimension (1D) nanocomposites. Numerous theoretical studies have revealed that magnetic properties of magnetic nanocomposites are strongly dependent on the preparation process and microstructure, such as grain size, dimension, distribution and magnetic interactions nature of soft- and hard-phases. These factors are inevitably affected by the annealing temperature. Therefore, the preparation process and

properties study of 1D soft/hard magnetic nanocomposites are important not only from a fundamental point of view but also for their potential technological applications. Among various 1D nanoshapes, nanocrystalline fibers are particularly being explored due to their strong shape anisotropy and spatial confinement effect, which are significant different from those of their bulk and particle counterparts [13].

Herein, we report on the structure and magnetic properties of nanocrystalline $\text{Ni}_{0.8}\text{Zn}_{0.2}\text{Fe}_2\text{O}_4$ (NZFO)/ $\text{SrFe}_{12}\text{O}_{19}$ (SFO) magnetic fibers. The magnetic fibers were synthesized by sol-gel spinning technique and subsequent annealing. The influence of annealing temperature on the microstructure, morphology and magnetic behavior of NZFO/SFO composite fibers is presented and discussed. The results obtained provide an important understanding of the relationship between annealing temperature and exchange coupling behavior in nanocrystalline NZFO/SFO composite fibers.

2. Experimental

2.1 Fiber preparation

Nanocrystalline $\text{Ni}_{0.8}\text{Zn}_{0.2}\text{Fe}_2\text{O}_4$ (NZFO)/ $\text{SrFe}_{12}\text{O}_{19}$ (SFO) composite fibers were prepared using the sol-gel spinning technique. The starting reagents were analytical grade nickel (II) acetate tetrahydrate ($\text{Ni}(\text{OCOCH}_3)_2 \cdot 4\text{H}_2\text{O}$), zinc acetate dihydrate ($\text{Zn}(\text{CH}_3\text{COO})_2 \cdot 2\text{H}_2\text{O}$), strontium (II) nitrate ($\text{Sr}(\text{NO}_3)_2$), iron(III) nitrate nonahydrate ($\text{Fe}(\text{NO}_3)_3 \cdot 9\text{H}_2\text{O}$) and citric acid ($\text{C}_6\text{H}_8\text{O}_7 \cdot \text{H}_2\text{O}$). Precursor solutions of composite were prepared according to the stoichiometric ratio by adding the raw materials to distilled water under stirring. Then citric acid was added to the above solution, the molar ratio of citrate radicals to metal ions was 1.5:1. The final solution was magnetically stirred for 24 h at room temperature and was transferred into a rotary

evaporator. The solution was evaporated in a vacuum at 60–70 °C to remove surplus water until a viscous liquid (gel) was obtained. The NZFO/SFO gel was spun the precursor fiber using a domestic micro/nano fiber spinning unit (Fig.1). The as-spun fibers were dried at 120 °C for 12 h, and then were annealed at different temperatures for 2 h in air. Nanocrystalline NZFO/SFO ferrite fibers were obtained. For comparison, single phase $\text{Ni}_{0.8}\text{Zn}_{0.2}\text{Fe}_2\text{O}_4$ and $\text{BaFe}_{12}\text{O}_{19}$ ferrite fibers were also synthesized.

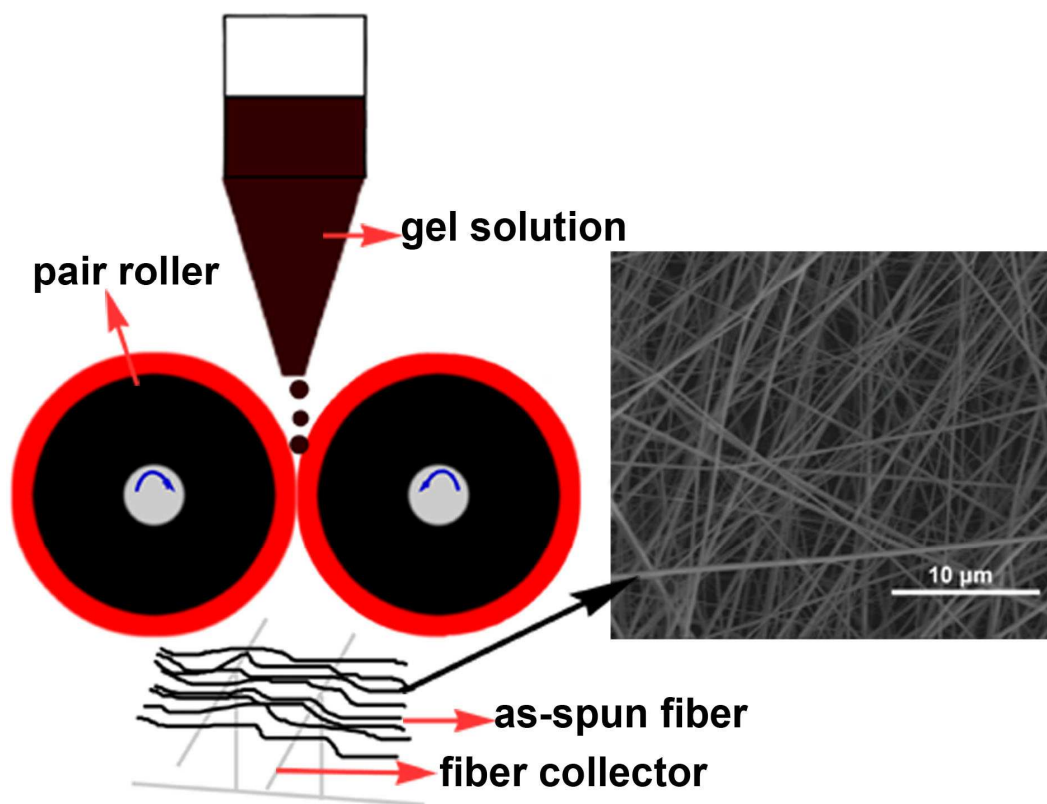


Fig. 1. Schematic diagram of sol-gel spinning apparatus

2.2 Characterization

The phases structure of the products were collected on a BrukerD8 Advance X-ray diffractometer (Cu $K\alpha$ radiation, $\lambda = 0.15406$ nm, Japan) in a 2θ range from 25° to 65° at room temperature. The morphologies of the as-synthesized products were examined by field-emission scanning electron microscopy (FESEM, JEOL, JSM-7001F, Japan). To further confirm the grain

size and chemical composition of the samples, the transmission electron microscopy (TEM) and energy-dispersive X-ray spectrometer (EDAX) measurements were carried out on JEM-2100 and Oxford INCA, respectively. The magnetic properties and exchange couple behavior of the resultant fibers were evaluated at room temperature using a vibrating sample magnetometer (VSM, HH-15) with applied magnetic field of up to $1194 \text{ kA}\cdot\text{m}^{-1}$ (15kOe), the samples for magnetic measurement were prepared using randomly oriented fiber, which were weighed for calculate of magnetic properties.

3. Results and discussion

3.1 Crystal structures

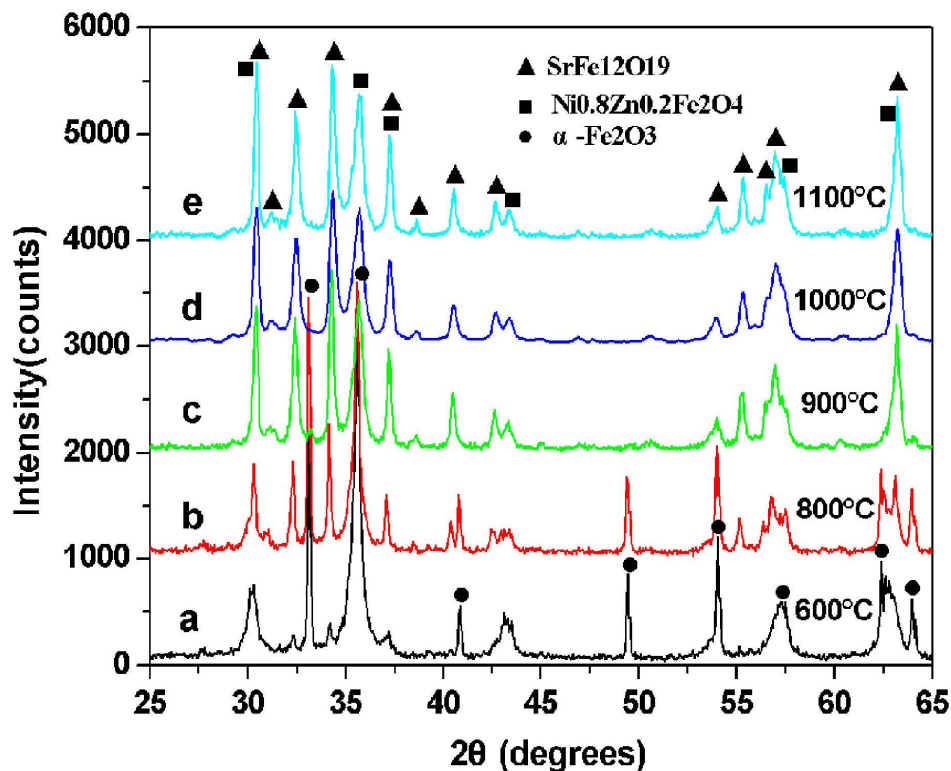


Fig. 2. XRD patterns of NZFO/SFO ferrite fibers annealed at different temperatures with molar ratio of 3:7

Fig. 2 shows the crystalline structure of NZFO/SFO ferrite fibers annealed at different

temperatures. At 600 °C (Fig.2a), the diffraction peaks are mainly indexed to NZFO phase (JCPDS 52-0277) and α -Fe₂O₃ phase (JCPDS 33-0664), and only trace amounts of SFO phase (JCPDS 33-1340) can be detected. This indicates that target NZFO/SFO ferrite can not be achieved under this annealing condition. Heating the sample to 800 °C (Fig.2b), the figure in XRD pattern clearly shows that peak intensity of SFO phase become sharper, and that of α -Fe₂O₃ phase becomes weak. This should be due to the nucleation and growth of SFO grains. With further increasing temperature to 900 °C or higher (Figs. 2c and d), all diffraction peaks observed match well with spinel NZFO phase and magnetoplumbite SFO phase, indicating that pure phase NZFO/SFO ferrite fibers are successfully obtained. Furthermore, the sharp and strong diffraction peaks also suggest that the as-obtained NZFO/SFO ferrite fibers are well crystallized. The average crystallite size (*D*) of NZFO phase and SFO phase in composite fibers calculated by using Debye-Scherrer's equation are shown in Table 1. The results suggest that the grain size grows continuously with increasing the annealing temperature, and also the grain growth rate of SFO phase is superior to that of NZFO phase.

Table 1 Average crystallite size (*D*) of nanocrystalline NZFO/SFO ferrite fibers annealed at different temperatures for 2 h with molar ration of 3:7

Temperature (°C)	<i>D</i> _{NZFO} (nm)	<i>D</i> _{SFO} (nm)
600	9.78	—
800	13.89	11.34
900	15.57	22.76
1000	18.74	28.97
1100	26.21	35.23

3.2 Morphology analysis

Fig. 3 shows the SEM images of NZFO/SFO as-spun fibers and fibers annealed at different temperatures for 2 h. The as-spun fibers (Fig. 3a) appear a continuous 1D texture structure and smooth surface due to the amorphous nature of composite fibers. Each individual fiber is uniform in the cross section, and the average diameter of as-spun fibers is $1.5\pm 0.55\ \mu\text{m}$. After annealing at different temperatures, it can be seen that the continuous 1D structure and uniform diameter is still remained, this indicates that the annealing process does not destroy morphology of NZFO/SFO ferrite fibers. However, a relatively rough surface is also formed. This phenomenon is related to a dramatic change in crystal structure and grain size. In addition, it also can be seen from the SEM images, the diameter of fibers exhibits an obvious shrinkage compared with that of as-spun fibers, the average diameter of fibers is $1.0\pm 0.25\ \mu\text{m}$. The shrinkage should be mainly attributed to the decomposition of metal salts and citric acid as well as crystallization of NZFO/SFO ferrite phase. Furthermore, the fiber annealed at 600°C displays a closely packed structure comprised of irregular NZFO and $\alpha\text{-Fe}_2\text{O}_3$ grains (Fig.3a), though minor amount holes can be also observed. As the annealing temperature reaches 800°C (Fig. 3c), some hexagonal plate-like grains of SFO phase are observed. These SFO grains are partly embedded in the composite fibers and partly adsorbed on surface of the fibers. With further increase annealing temperature to 900°C or higher (Figs. 3d and 3e), more hexagonal plate-like grains are formed. Moreover, these grains begin closely packed, dense and self-organized to yield the fiber morphology. For this close-packed structure and morphology, a strong exchange spring behavior at the interfaces between soft NZFO phase and hard SFO phase can be expected. It is worth noting that NZFO and SFO grains are randomly stacked each other along the fiber

axis. Such result is obviously different from F. Z. Song's previous results, in which the soft grains adhere on the surface of SFO grains [14]. This phenomenon can be ascribed to the fact that the spinel structure of NZFO ferrite is similar to S blocks in the SFO ferrite, which results in well compatibility between the NZFO and SFO phase.

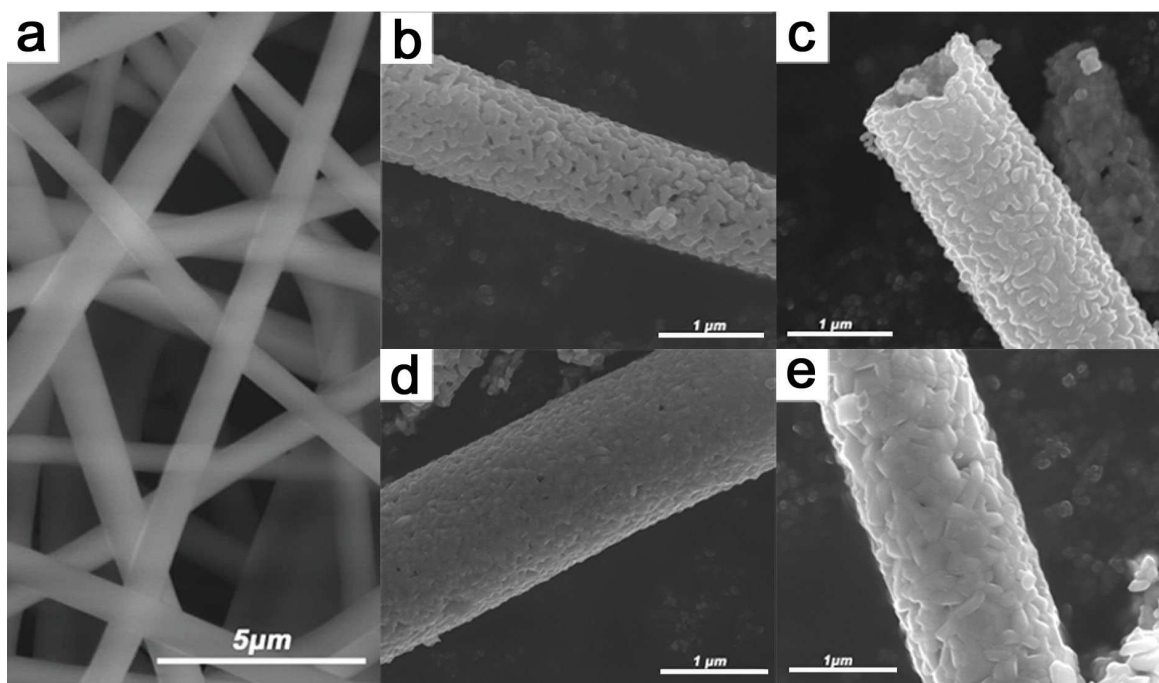


Fig. 3. SEM images of as-spun NZFO/SFO composite fibers and fibers annealed at different temperatures for 2 h (a) as-spun, (b) 600°C, (c) 800°C, (d) 900°C, (e) 1000°C

Fig.4 shows the TEM and EDAX images of NZFO/SFO ferrite fibers annealed at 900 °C. As can be seen from Figs.4a and 4b, the ferrite fibers are composed of rather dense irregular NZFO and hexagonal SFO nanograins. The average crystallite sizes are revealed to be about 15 nm and 20 nm for NZFO and SFO phase respectively, in agreement with the results of XRD. However, the small conjunction of nanograins is also observed in some regions due to the attractive forces among grains. The corresponding selected area electron diffraction (SAED) pattern (Fig.4c) displays clear spotty rings, suggesting polycrystalline structure characteristic of

NZFO/SFO ferrite fiber. Diffraction rings from both soft NZFO phase and hard SFO phase can be clearly observed in the figure, which confirms the coexistence of magnetically soft NZFO and hard SFO phase. The results of EDAX analysis (Fig.3d) shows that the composite fibers are composed of Ni, Zn, Sr, Fe and O. And the chemical compositions obtained are basically consistent with the designed composition.

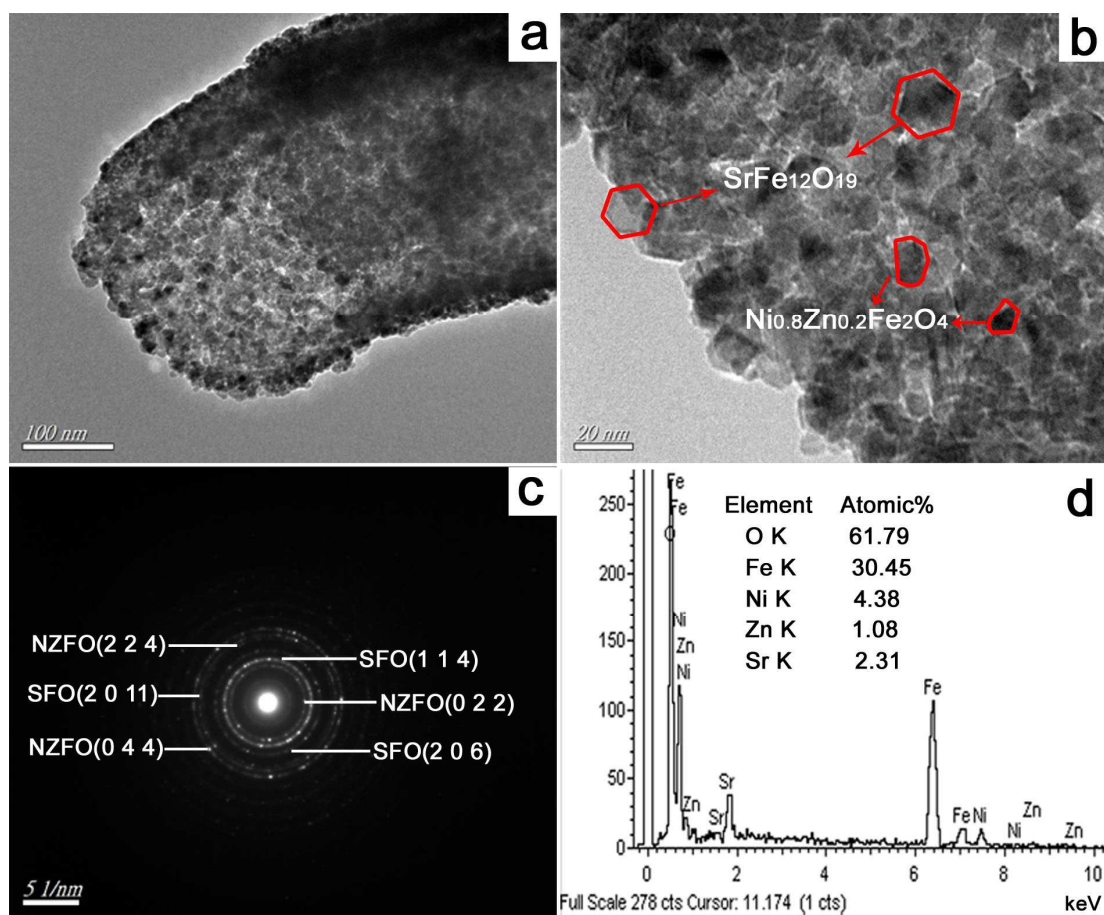


Fig. 4. TEM images (a, b), SAED pattern (c) and EDAX spectrum (d) of NZFO/SFO ferrite fibers annealed at 900°C for 2 h with molar ratio of 3:7

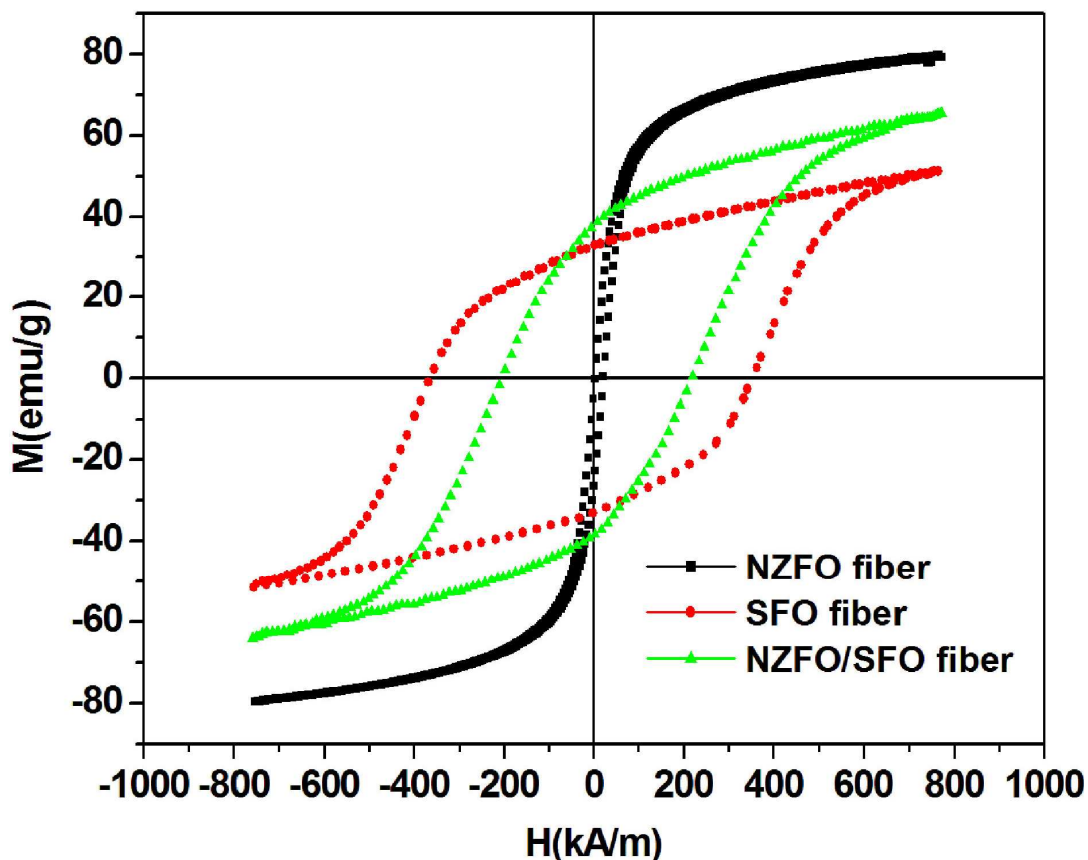


Fig. 5. Hysteresis loops at room temperature of single phase $\text{Ni}_{0.8}\text{Zn}_{0.2}\text{Fe}_2\text{O}_4$, $\text{SrFe}_{12}\text{O}_{19}$ fiber and nanocrystalline NZFO/SFO composite fiber with molar ratio 3:7

3.3 Magnetic properties

Fig. 5 depicts the hysteresis loops of single phase NZFO fiber, SFO fiber and nanocrystalline NZFO/SFO composite fiber annealed at 1000 °C for 2 h with molar ratio 3:7. Room temperature magnetic parameters (M_s , H_c , and M_r/M_s) derived from hysteresis loops are determined and presented in Table 2. From the Fig. 5 and Table 2, all the samples exhibit ferromagnetic-like behavior at room temperature. Maximum magnetizations (M_s) of single phase NZFO and SFO ferrite fibers are 79.64 emu/g and 50.44 emu/g, and the corresponding values of coercivity (H_c) are 11.08 kA/m and 360.64 kA/m, respectively. Evidently, the H_c of NZFO and SFO ferrite fibers differs by orders of magnitude, which reveals intrinsic soft and hard magnetic

properties of respective ferrites. For the nanocrystalline NZFO/SFO composite fibers, despite consisting of soft and hard phases, the hysteresis loop shows a single-phase-like magnetic behavior (no steps). This implies the soft and hard magnetic phases are well exchange coupled to each other. If there is no exchange coupling between soft and hard magnetic phases, then the saturation magnetization of nanocomposite fibers can be predicted as [15]:

$$M_s = M_{s,h}(1 - f_s) + M_{s,s}f_s \quad (1)$$

Where, $M_{s,h}$, $M_{s,s}$ are the saturation magnetization of hard SFO phase and soft NZFO phase, respectively, and f_s is the weight fraction of the soft phase. However, according to Equation (1), the predicted M_s value of 52.98 emu/g for NZFO/SFO composite fibers is lower than 63.98 emu/g measured. And the measured M_r/M_s ratio of 0.60 for the NZFO/SFO composite fibers is larger than the value of 0.5 predicted for non-interacting permanent magnets. Generally, remanence enhancement effect and single phase demagnetization curve are not only the characteristic of two phase nanocrystalline composite magnets, but also are important in judging the exchange spring [16, 17]. Thus, above results further demonstrate that the intimate contact between the NZFO and SFO grains leads to an effective interfacial exchange coupling. The exchange coupling effect results in cooperative magnetization switching of the two phases.

Table 2 The magnetic parameters (M_s , H_c , and M_r/M_s) of single phase NZFO fiber, SFO fiber and nanocrystalline NZFO/SFO composite fiber at 1000 °C

Sample	M_s (emu/g)	H_c (kA/m)	M_r/M_s
NZFO	79.64	11.08	0.33
SFO	50.44	360.64	0.65
NZFO/SFO	63.98	212.71	0.60

As we know, the exchange spring behavior of the soft/hard magnetic nanocomposites strongly depends on various factors, including the distribution of the magnetically soft and hard phases, the average grain sizes of the individual phase and the particle shape, etc. These factors may be determined by annealing temperature to some extent. Thus we investigate magnetic properties of nanocrystalline NZFO/SFO ferrite fibers obtained at different temperatures. Fig.6 illustrates the hysteresis loops of nanocrystalline NZFO/SFO composite fibers at different annealing temperature. From Fig. 6, the sample annealed at 600 °C exhibits a similar hysteresis loop with soft magnetic materials, suggesting the NZFO phase in composite fiber is dominating. It also should be noted that the value of M_s is far smaller than the pure NZFO phase. This is mainly due to the existence of non-magnetic $\alpha\text{-Fe}_2\text{O}_3$ phase in agreement with the results of XRD, which reduce the magnetic moment of NZFO phase. After sample annealed at 800 °C, the sample has a two-step hysteresis loop, indicating non-complete exchange coupling between soft and hard grains. As the annealing temperature reaches 900 °C, the sample exits a smooth single-phase-like hysteresis loop, implying occurrence of effective exchange coupling between NZFO phase and SFO phase. This is due to the fact the thermal energy is high enough to overcome the energy barrier for the occurrence of exchange coupling interaction, leading to the sufficient exchange coupling at the interfaces between the soft and hard phase. According to the exchange coupling model of Kneller and Hawig [18], effective exchange coupling can be obtained only if the dimension of the soft phase is not larger than a critical length which is typically twice or less than the domain wall width of the hard phase. The typical domain wall width of the hard $\text{SrFe}_{12}\text{O}_{19}$ ferrite is approximately 10 nm [6]. Grain size of the NZFO ferrite in samples annealed at 900 °C and 1000 °C are in range of 10-20 nm as shown in Table 1, which

meet the condition for optimum exchange spring behavior. Hence, the switching of the soft and hard phase should indeed occur coherently, leading to a smooth magnetization transition. However, as the annealing temperature increase to 1100 °C, the hysteresis loop exhibits a constrictive tendency in the second quadrant. It can most likely be due to the point that the larger soft phase regions are formed owing to conjunction of soft grains at higher temperature. This phenomenon does not allow intergrain exchange coupling to suppress the diolar interaction in the center of soft regions which causes the appearance of the magnetic vortex state [19].

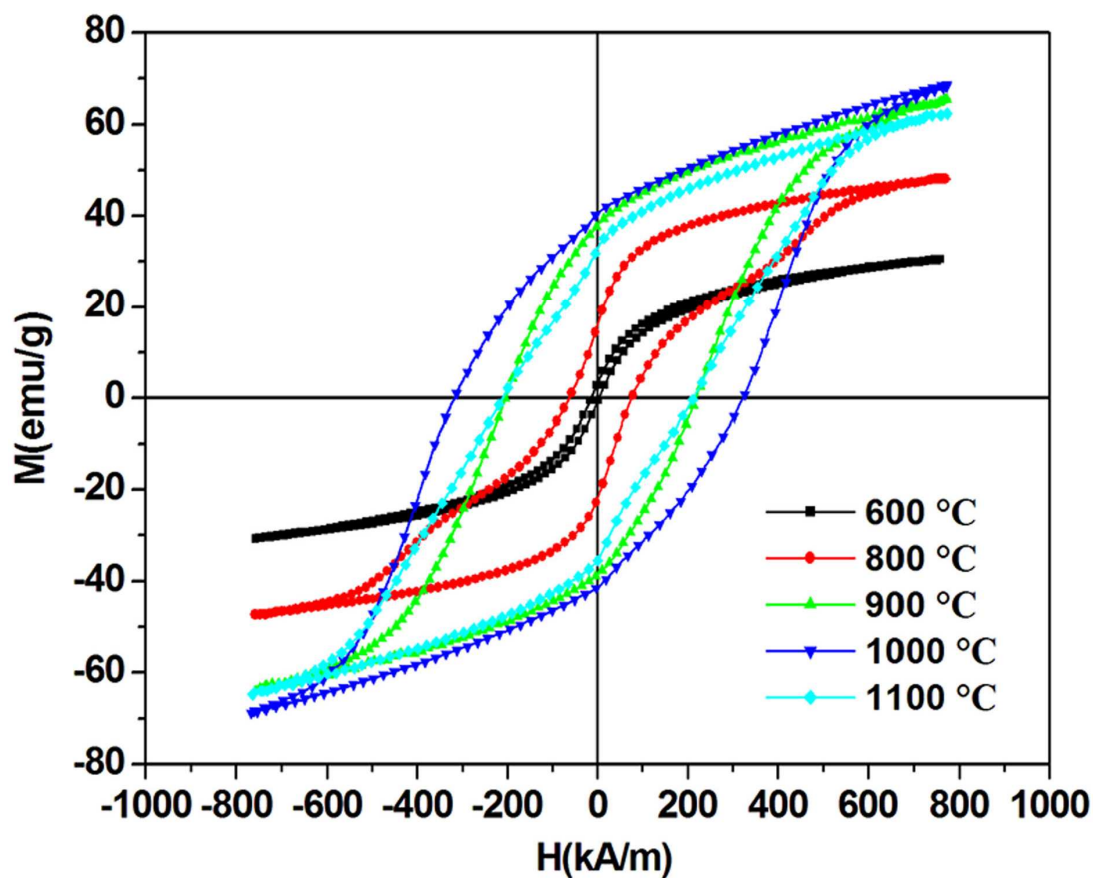


Fig. 6. Hysteresis loops at room temperature of nanocrystalline NZFO/SFO composite fibers annealed at different temperatures for 2 h

Table 3 The magnetic parameters (M_s , M_r , H_c and M_r/M_s) of nanocrystalline NZFO/SFO ferrite fibers annealed at different temperatures for 2 h with molar ratio of 3:7

Temperature (°C)	M_s (emu/g)	M_r (emu/g)	H_c (kA/m)	M_r/M_s
600	30.99	2.02	9.19	0.07
800	48.15	18.87	69.79	0.39
900	63.98	38.24	212.71	0.60
1000	67.02	41.38	318.85	0.62
1100	63.11	34.23	208.53	0.54

In order to further examine the exchange coupling behavior between NZFO and SFO phases, magnetic parameters of NZFO/SFO composite fibers are calculated and listed in Table 3. It can be seen from Table 3, the M_s value of NZFO/SFO composite fibers initially increases with increasing annealing temperature from 600 °C to 800 °C even though non-complete exchange coupling. And the H_c and M_r exhibit similar tendency from M_s value. The main reasons are the reduction of α - Fe_2O_3 phase and formation of SFO phase as discussed in XRD, which enhance the surface magnetic moments of soft NZFO grains and increase the amount of hard SFO grains. As the annealing temperature increases to 900 °C, there exists an effective interfacial exchange coupling between NZFO and SFO grains, which has been confirmed by the hysteresis loops. The values of M_s , H_c and M_r increase gradually and reach their maximum values of 67.02 emu/g, 318.85 kA/m, and 41.38 emu/g at 1000 °C, respectively. This is mainly related to magnetic interactions between soft and hard phases. Because the composite ferrite fibers are mixture of the soft (NZFO) and hard (SFO) phases, there are two main magnetic interactions, exchange coupling and dipolar interactions that determine the extent of the exchange interaction in the

isotropic nanocomposite fiber. When composite ferrite fibers are annealed at appropriate temperature, the grain sizes less than the critical length can be achieved. Based on the micromagnetic modeling, the dipolar interaction can be neglected. Magnetization distribution in the remanence state is only determined by the exchange interaction and magnetocrystalline anisotropy [20]. If an external magnetic field is applied, there will be a competition between the magnetocrystalline energy, the exchange interaction, and the interaction between the applied field and the spins of the nanocomposite fibers. The soft phase will be easily aligned in the direction of the applied field due to the smaller magnetocrystalline anisotropy energy compared to hard SFO phase. However, when the soft NZFO phase is sufficiently exchange coupled with the neighboring hard SFO phase, the SFO phase will couple the magnetic moments of NZFO phase by strong exchange interaction and try to align in its own easy direction. Therefore, it is arduous that the atomic magnetic moment in the soft phase is aligned in the direction of the applied field, which leads to the increase of all the magnetic properties. It is important to note that the nanocrystalline NZFO/SFO composite fibers studied in this work have a much higher magnetic properties compared to their nanoparticle counterparts reported previously [11]. This may be attributed to large shape anisotropy effect of composite fibers besides the exchange coupling of two phases. However, with further increase the annealing temperature to 1100 °C, the magnetic properties start deterioration. This is mainly related to the growth of ferrite grains. Firstly, grain growth leads to grain size of soft NZFO phase exceeding the requirement of the exchange coupling on grain size. Secondly, grain growth gives rise to conjunction each other among soft magnetic grains and forms the large soft magnetic region. As a result, the exchange coupling interaction can not suppress the dipolar interaction in the soft phase which leads to the

appearance of magnetic vortex state, and therefore deteriorates exchange coupling between soft NZFO and hard SFO phases.

The results discussed above show that the nanocrystalline NZFO/SFO composite fibers annealed at optimized conditions can simultaneously combine the magnetic characteristic of soft phase with high specific saturation magnetization and hard phase with high coercivity. Such novel magnetic composite fibers will be more technologically important in future.

4. Conclusions

In conclusion, nanocrystalline NZFO/SFO composite fibers can be readily synthesized using the sol-gel spinning technique followed by annealing. The effects of the annealing temperature on the crystalline structure, magnetic properties and exchange coupling behavior of NZFO/SFO composite fibers have been studied systematically. Phase structure and morphology analysis show that the two-phase NZFO/SFO nanocomposite fibers can be obtained at above 900 °C. Moreover, the annealing temperature plays an important role for exchange coupling behavior between soft and hard magnetic phases. As the annealing temperature increase to 900 °C, the NZFO/SFO composite fibers exhibit single-phase-like magnetic behavior, indicating the soft NZFO phase and hard SFO phase are well exchange coupled. Additionally, the exchange coupling interaction can be tuned by changing the annealing conditions. Thus, we believe that nanocrystalline NZFO/SFO composite fibers can combine the high M_s of soft NZFO ferrite and large H_c of hard SFO ferrite, and have potential applications such as electromagnetic interference, nanodevices and nanomembrance.

Acknowledgements

This work was supported by National Natural Science Foundation of China (NO.51202091),

The Natural Science Foundation of Jiangsu Province (NO.BK20141300) and China Postdoctoral Science Foundation (NO.2013M541612).

Reference

- [1] D. Roy, P. S. Anil Kumar, Enhancement of $(BH)_{\max}$ in a hard-soft-ferrite nanocomposite using exchange spring mechanism. *J. Appl. Phys.*, 2009, 073902, 106-110.
- [2] R. Skomski, J. M. D. Coey, Giant energy product in nanostructured two-phase magnets, *Phys. Rev. B*, 1993, 48, 15812-15816.
- [3] J.E. Davies, O. Hellwiga, E.E. Fullerton, Anisotropy dependence of irreversible switching in Fe/SmCo and FeNi/FePt exchange spring magnet films. *Appl. Phys. Lett.*, 2005, 86, 262501–262503
- [4] Z. J. Guo, J. S. Jiang, J. E. Pearson, S. D. Bader, J. P. Liu, Exchange-coupled Sm–Co/Nd–Co nanomagnets: correlation between soft phase anisotropy and exchange field. *Appl. Phys. Lett.*, 2002, 81(11), 2029–2031.
- [5] W. Liu, Z.D. Zhang, J.P. Liu, L.J. Chen, L.L. He, Y. Liu, X.K. Sun, D.J. Sellmyer, Exchange coupling and remanence enhancement in nanocomposite multilayer magnets. *Adv. Mater.*, 2002, 14, 1832–1834.
- [6] S. Tyagi, H.B. Baskeyb, R.C. Agarwalaa, V. Agarwalaa, T.C. Shami, Development of hard/soft ferrite nanocomposite for enhanced microwave absorption. *Ceram. Int.*, 2011, 37, 2631–2641.
- [7] P. Saravanan, Jen-Hwa Hsu, G. L. N. Reddy, Sanjiv Kumar, S.V. Kamat, Annealing induced compositional changes in SmCo₅/Fe/SmCo₅ exchange spring trilayers and its impact on magnetic properties. *J. Alloy. Compd.*, 2013, 574, 191–195.

- [8] J. Zhang, Y. K. Takahashi, R. Gopalan, K. Hono, Sm(Co,Cu)/Fe exchange spring multilayer films with high energy product, *Appl. Phys. Lett.* 2005, 86, 122509–122515.
- [9] G. K. Thompson, B. J. Evans, Magnetic properties, compositions, and microstructures of high-energy product strontium hexaferrites. *J. Appl. Phys.*, 1990, 67, 4601–4608.
- [10] W. Rodewald, B. Wall, M. Katter, K. Uestuener, Top Nd-Fe-B magnets with greater than 56 MGOe energy density and 9.8 kOe coercivity, *IEEE Trans. Magn.*, 2002, 38, 2955-3002.
- [11] D. Roy, C. Shivakumara, P. S. Anil Kumar, Observation of the exchange spring behavior in hard–soft-ferrite nanocomposite. *J. Magn. Magn. Mater.* , 2009, 321, L11–L14.
- [12] S. Manjura Hoque, C. Srivastava, V. Kumar, N. Venkatesh, H.N. Das, D.K. Saha, K. Chattopadhyay, Exchange-spring mechanism of soft and hard ferrite nanocomposites. *Mater. Res. Bull.*, 2013, 48, 2871–2877.
- [13] J. Xiang, X. H. Zhang, J. L. Li, Y. Q. Chu, X. Q. Shen, Fabrication, characterization, exchange coupling and magnetic behavior of CoFe₂O₄/CoFe₂ nanocomposite nanofibers. *Chem. Phys. Lett.*, 2013, 576, 39–43.
- [14] F. Z. Song, X. Q. Shen, M. Q. Liu, J. Xiang, Magnetic hard/soft nanocomposite ferrite aligned hollow microfibers and remanence enhancement. *J. Colloid Interf. Sci.*, 2011, 354, 413–416.
- [15] K.W. Moon, S.G. Cho, Y.H. Choa, K.H. Kim, J. Kim, Synthesis and magnetic properties of nano Ba-hexaferrite/NiZn ferrite composites, *Phys. Status Solidi A*, 2007, 204, 4141–4144.
- [16] D. T. M. Hue, P. Lampen, T. V. Manh, V. D. Viet, H. D. Chinh, H. Srikanth, M. H. Phan. Synthesis, structure, and magnetic properties of SrFe₁₂O₁₉/La_{1-*x*}Ca_{*x*}MnO₃ hard/soft phase composites. *J. Appl. Phys.*, 2013, 114, 123901–123906.

- [17] Y. Wang, Y. Huang, Q. F. Wang. Preparation and magnetic properties of $\text{BaFe}_{12}\text{O}_{19}/\text{Ni}_{0.8}\text{Zn}_{0.2}\text{Fe}_2\text{O}_4$ nanocomposite ferrite. *J. Magn. Magn. Mater.*, 2012, 324, 3024–3028.
- [18] E.F. Kneller, R. Hawig, The exchange-spring magnet: a new material principle for permanent magnets. *IEEE. Trans. Magn.*, 1991, 27, 3588–3600.
- [19] M.A. Radmanesh, S.A. Seyyed Ebrahimi, Synthesis and magnetic properties of hard/soft $\text{SrFe}_{12}\text{O}_{19}/\text{Ni}_{0.7}\text{Zn}_{0.3}\text{Fe}_2\text{O}_4$ nanocomposite magnets. *J. Magn. Magn. Mater.*, 2012, 324, 3094–3098.
- [20] C. B. Rong, H. W. Zhang, R. J. Chen, S. L. He, B. G. Shen, The role of dipolar interaction in nanocomposite permanent magnets. *J. Magn. Magn. Mater.*, 2006, 302, 126–136.